Rayleigh waves for a discrete elastic paraxial equation

G. W. Hedstrom
Lawrence Livermore National Laboratory, P. O. Box 808, L-321, Livermore, California 94550
(Received 8 September 1992; revised manuscript received 6 August 1993)

We investigate the effects of a free surface on the 45° paraxial equation for linear elasticity in a half space. We show that the 45° equation has no Rayleigh wave and that it has an exponentially growing instability. We also examine a standard finite-difference approximation to the elastic paraxial equation. We show that the discrete equation also has an exponential instability, but this may be removed by projection. We also find that the discrete elastic paraxial equation has no Rayleigh waves when the mesh size is small, but a coarse mesh gives two Rayleigh waves. Moreover, by a proper choice of the mesh sizes, we may select a discretization so that one of these discrete Rayleigh waves has the speed of a physical Rayleigh wave, and we may project out the nonphysical discrete Rayleigh wave.

PACS number(s): 02.70.−c, 02.60.−x, 91.30.Fn

I. INTRODUCTION

We describe some results on Rayleigh waves for a paraxial (one-way-wave) approximation to the equation of linear elasticity, and we examine a finite-difference approximation. In acoustics and electromagnetics a paraxial equation is a good approximation for tracking waves in a particular direction if the sound speed or refractive index is slowly varying. Elasticity is more complicated in that we have two wave speeds, compressional waves (P waves) are faster than torsional waves (S waves). We therefore have to decide whether to use a paraxial equation capable of tracking both S and P waves or to track only one type of wave. This choice depends to some extent on the particular application. Thus, in exploration seismology Claerbout [1] uses an elastic paraxial equation which tracks only upgoing P waves. Other authors, such as Graves [2] and Wapenaar [3] track both S and P waves. Our interest is in long-range seismology so we also track both kinds of waves, and we choose a paraxial equation which tracks in a horizontal direction.

The problem we deal with arises from the effects of a free surface. Specifically, there may be Rayleigh waves in a boundary layer next to the free surface, and they travel more slowly than S waves. It is therefore natural to ask how good a job a paraxial equation designed to track S and P waves will do in approximating a Rayleigh wave. The work of Graves [2] suggests that there may be trouble. We select one commonly used elastic paraxial equation (the 45° equation) in two spatial dimensions, and we track both S and P waves horizontally. We show that there is indeed trouble: this paraxial equation has no Rayleigh waves, and it is unstable.

One might try to rectify this situation by changing either the paraxial equation or the boundary conditions at the free surface (or both). Here, we take a different approach, working with a finite-difference approximation to the elastic paraxial equation. We investigate a standard central-difference approximation to the horizontal elastic 45° equation, and we show that for an incompressible elastic material one may obtain a variety of surface-wave behaviors by a proper selection of the mesh sizes in the horizontal and vertical directions. It should not be surprising that the difference scheme is unstable, but we can remove the unstable growth by a projection. We also find that, depending on the horizontal and vertical mesh sizes, there are zero or two Rayleigh waves (or at the transition only one), and the speeds of these discrete Rayleigh waves depend very strongly on the mesh sizes. With a careful choice of the mesh sizes it is possible to obtain a Rayleigh wave with the same velocity as a physical Rayleigh wave.

From the point of view of linear algebra what is going on here is that the difference scheme may be represented as an iteration of the unknowns V_n at one horizontal position x_n from the previous unknowns V_{n-1}

$$\mathcal{N}V_n = \mathcal{M}V_{n-1}, \tag{1}$$

with matrices $\mathcal{M}$ and $\mathcal{N}$ determined by the difference scheme. A discrete Rayleigh wave is an eigenvector V

$$\xi\mathcal{N}V = \mathcal{M}V \tag{2}$$

with an eigenvalue ξ such that $|\xi| = 1$, and an unstable mode corresponds to an eigenvalue $|\xi| > 1$. The iteration (1) is equivalent to the power method for finding the eigenvalue with largest absolute value [4], and in our case it finds the unstable mode very quickly. We may remove this instability, as well as the nonphysical discrete Rayleigh wave, by deflation [4].

II. THE ELASTIC EQUATIONS

We consider a linear elastic solid with constant Lamé parameters λ and μ and constant density ρ. The P-wave speed α and the S-wave speed β are then given by

$$\alpha^2 = \frac{\lambda + 2\mu}{\rho} \quad \text{and} \quad \beta^2 = \frac{\mu}{\rho}.$$

We also introduce the parameter

$$q = \frac{\beta}{\alpha}. \tag{3}$$

In order to reduce the number of parameters, in our discussions later we impose the incompressibility condition $\lambda = \mu$, which in terms of q takes the form

$$q = \frac{1}{\sqrt{3}}. \tag{4}$$

We remark that we find it more convenient to express the material properties in terms of q than in terms of the Poisson ratio $\sigma = \lambda/(2\lambda+2\mu)$, although there is a simple relationship between them

$$\sigma = \frac{1-2q^2}{2(1-q^2)}.$$

We also note that for a solid we have $\mu > 0$ and $\lambda + 2\mu/3 > 0$, so that the value of q is restricted to the interval

$$0 < q < 1.$$

We write the elastic equations in terms of dilatation and shear potentials as in Hudson [5]. In the absence of sources the equations of linear plane elasticity take the form

$$\partial_t^2\phi = \alpha^2(\partial_x^2 + \partial_z^2)\phi, \tag{5a}$$
$$\partial_t^2\psi = \beta^2(\partial_x^2 + \partial_z^2)\psi \tag{5b}$$

in a homogeneous medium. The displacement (u_x, u_z) is then given by

$$u_x = \partial_x\phi + \partial_z\psi, \tag{6a}$$
$$u_z = \partial_z\phi - \partial_x\psi. \tag{6b}$$

We work with the Fourier transform of (5) with respect to time,

$$-\omega^2\phi = \alpha^2(\partial_x^2 + \partial_z^2)\phi, \tag{7a}$$
$$-\omega^2\psi = \beta^2(\partial_x^2 + \partial_z^2)\psi. \tag{7b}$$

The elastic solid is assumed to occupy the two-dimensional half space $-\infty < x < -\infty$, $z > 0$. The boundary conditions at the free surface $z = 0$ are the normal components of the traction vanishing, leading to [5]

$$2\,\partial_x\partial_z\phi - (\partial_x^2 - \partial_z^2)\psi = 0, \tag{8a}$$
$$\left[(1-2q^2)\partial_x^2 + \partial_z^2\right]\phi - 2q^2\,\partial_x\partial_z\psi = 0. \tag{8b}$$

III. RAYLEIGH WAVES

A Rayleigh wave is a modal solution to (7) and (8) of the form

$$\phi = A\exp\{ikx - \nu_\alpha z\}, \qquad \psi = B\exp\{ikx - \nu_\beta z\}, \tag{9}$$

where k, ν_α, and ν_β are positive. If we substitute (9) into (7), we obtain the dispersion relations

$$\nu_\alpha = \sqrt{k^2 - \frac{\omega^2}{\alpha^2}}, \qquad \nu_\beta = \sqrt{k^2 - \frac{\omega^2}{\beta^2}}. \tag{10}$$

Because ν_α and ν_β are homogeneous in k and ω, we introduce the parameter s defined by

$$s = \frac{\omega}{k\beta}, \tag{11}$$

so that the dispersion relations (10) take the form

$$\frac{\nu_\alpha}{k} = \sqrt{1-q^2s^2}, \qquad \frac{\nu_\beta}{k} = \sqrt{1-s^2}. \tag{12}$$

We remark that s may be viewed as the ratio of speeds: the phase velocity ω/k divided by the S-wave speed β. We also remark that the restrictions that $k > 0$ and that ν_β be real and positive imply that

$$0 < s < 1. \tag{13}$$

In particular, we exclude $s = 0$ since it occurs only at one frequency, $\omega = 0$.

Substitution of the trial solution (9) into (8) yields a matrix equation which has nontrivial solutions if and only if

$$F_q(s) = \left(\frac{2\nu_\alpha^2}{k^2} + (2q^2-1)s^2\right)\left(\frac{2\nu_\beta^2}{k^2} + s^2\right) - 4\frac{\nu_\alpha\nu_\beta}{k^2} = 0. \tag{14}$$

Thus by (12), the speed of a Rayleigh wave relative to the S-wave speed is a zero of

$$F_q(s) = (2-s^2)^2 - 4\sqrt{(1-q^2s^2)(1-s^2)} \tag{15}$$

such that $0 < s < 1$. A graph of F_q for $q = 1/\sqrt{3}$ is shown in Fig. 1, and we see that it has a single positive zero. As mentioned earlier, the root at $s = 0$ has no physical interest.

IV. THE 45° EQUATION

There are many versions of paraxial approximations to (5). See Wapenaar [3], for examples. We discuss the one which is a 45° approximation for both P and S waves,

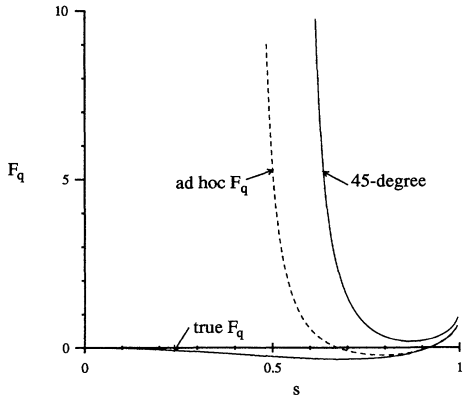

FIG. 1. Rayleigh functions.

$$\left(1+\frac{\alpha^2}{4\omega^2}\,\partial_z^2\right)\partial_x\phi = i\omega\left(\frac{1}{\alpha}+\frac{3\alpha}{4\omega^2}\,\partial_z^2\right)\phi, \tag{16a}$$

$$\left(1+\frac{\beta^2}{4\omega^2}\,\partial_z^2\right)\partial_x\psi = i\omega\left(\frac{1}{\beta}+\frac{3\beta}{4\omega^2}\,\partial_z^2\right)\psi. \tag{16b}$$

The paraxial equation (16) is chosen so as to be an accurate approximation to waves propagating in the direction of the positive x axis.

If we substitute the modal solution (9) into (16), we find that in terms of the parameters q and s the dispersion relation for the 45° equation is

$$\frac{\nu_\alpha}{k} = 2qs\sqrt{\frac{1-qs}{3qs-1}}, \qquad \frac{\nu_\beta}{k} = 2s\sqrt{\frac{1-s}{3s-1}}. \tag{17}$$

Note that if $\omega = 0$, the mappings (17) are trivial, $\nu_\alpha = \nu_\beta = 0$ for all k. We therefore again restrict our attention to $s \neq 0$. It is clear that in order for both ν_α and ν_β to be real for real s, we must have

$$\frac{1}{3} < q < 1 \quad \text{and} \quad \frac{1}{3q} < s < 1.$$

The analogue of the Rayleigh function (15) is obtained by substituting ν_α and ν_β from (17) into (14) to get

$$F_q(s) = \left(\frac{8q^2s^2(1-qs)}{3qs-1} + (2q^2-1)s^2\right) \times \left(\frac{8s^2(1-s)}{3s-1} + s^2\right) - 16qs^2\sqrt{\frac{(1-qs)(1-s)}{(3qs-1)(3s-1)}}. \tag{18}$$

The graph of this function is shown in Fig. 1 for the case of an incompressible solid $q = 1/\sqrt{3}$, and we see that there are no real zeros other than $s = 0$. That is, the 45° equation (16) has no Rayleigh waves.

V. REMARKS

The great difference between the Rayleigh function for the elastic wave equation (7) and the Rayleigh function for the 45° equation is closely tied to the fact that Rayleigh waves are incompatible with the assumptions behind (16). In fact, (16a) represents horizontal P waves moving at speed α ($s = 1/q$), and (16b) represents horizontal S waves moving at speed β ($s = 1$). In particular, the differential equation (16) is chosen so that the behavior of ν_β/k in (17) as $s \to 1$ is that

$$\frac{\nu_\beta}{k} = \sqrt{2(1-s)}\left\{1 - \frac{1-s}{4} + O((1-s)^2)\right\}, \tag{19}$$

in agreement with the behavior of ν_β/k for the wave equation (12). Corresponding agreement is obtained for the behavior of ν_α/k in (12) and (17) as $s \to 1/q$. No attempt is made in (16) to obtain agreement between (12) and (17) for the value $s = s_0$ corresponding to the speed of a Rayleigh wave, $F_q(s_0) = 0$ with F_q as given by (15).

One might think to rectify the situation by changing the paraxial equation in order to force it to have a correct Rayleigh wave. We therefore consider

$$\left(1+\frac{\gamma_\alpha\alpha^2}{\omega^2}\,\partial_z^2\right)\partial_x\phi = i\omega\left(\frac{1}{\alpha}+\frac{(\gamma_\alpha+0.5)\alpha}{\omega^2}\,\partial_z^2\right)\phi, \tag{20a}$$

$$\left(1+\frac{\gamma_\beta\beta^2}{\omega^2}\,\partial_z^2\right)\partial_x\psi = i\omega\left(\frac{1}{\beta}+\frac{(\gamma_\beta+0.5)\beta}{\omega^2}\,\partial_z^2\right)\psi \tag{20b}$$

with appropriate choices of γ_α and γ_β. We selected (20) for three reasons. One is that it reduces to (16) when $\gamma_\alpha = \gamma_\beta = 1/4$. Another is that (20) gives the traditional 15° equation when $\gamma_\alpha = \gamma_\beta = 0$. Finally, for any value of γ_β the dispersion relation for (20)

$$\frac{\nu_\beta}{k} = s\sqrt{\frac{1-s}{(\gamma_\beta+0.5)s-\gamma_\beta}} \tag{21}$$

satisfies a weak form of (19) as $s \to 1$, namely,

$$\frac{\nu_\beta}{k} \approx \sqrt{2(1-s)}.$$

One may choose the value of γ_β so as to obtain equality at the Rayleigh root s_0 between the value of ν_β given by (21) and the value (12) for the elastic wave equation. The value of γ_α may be chosen similarly to give the correct value of ν_α at the Rayleigh root. The Rayleigh function for (20) corresponding to these choices of the parameters is shown in Fig. 1 and is labeled "*ad hoc* F_q." We see that (as expected) the Rayleigh function for (20) has a zero at the Rayleigh root, but it also has another zero. Furthermore, it happens that (20) still has an instability excited by the free surface. We therefore take this approach no further.

Another explanation of the peculiarities we have observed is that paraxial equations are derived under the assumption of slow variation in directions tangent to a wave front, but the introduction of a free surface violates this assumption. It is therefore not so surprising that there may be difficulties with paraxial equations at a free surface.

VI. STABILITY OF THE 45° EQUATION

The problem we have for the 45° equation is an initial-boundary-value problem in the sense that initial data are prescribed at $x = 0$, and the solution propagates with increasing x, subject to a boundary condition at $z = 0$. There is an established stability theory, called the GKS theory, so named for the work of Gustafsson, Kreiss, and Sundström [6]. The clearest form of the theory is the reworking by Trefethen [7]. Trefethen's paper also gives many further references.

Since the worst instabilities correspond to modes (9) which grow in x while decreasing in z, the stability theory begins by studying (17) as conformal mappings of the region $\mathrm{Im}k < 0$ and seeing whether the images overlap with the half-planes $\mathrm{Re}\nu_\alpha > 0$ and $\mathrm{Re}\nu_\beta > 0$. In terms of the variable $s = \omega/(k\beta)$ defined in (11), the half-plane $\mathrm{Im}k < 0$ corresponds to the half-plane $\mathrm{Im}s > 0$. It is sufficient to investigate the mapping properties of

$$\nu_\beta = \frac{2\omega}{\beta}\sqrt{\frac{1-s}{3s-1}}, \tag{22}$$

since the factor q only changes the scale for ν_α. The mapping (22) is the composition of a fractional linear transformation

$$\eta = (1-s)/(3s-1) \tag{23}$$

with a square root $\nu_\beta = C\sqrt{\eta}$, where $C = 2\omega/\beta$. Both of these mappings are very well known. See Bieberbach [8].

Let us determine the image of the half-plane $\mathrm{Im}s > 0$ by the mapping (23). The boundary of this half-plane is a line which is therefore mapped onto a line or a circle. We find out what the image is by examining three points: $s = 0$, $1/3$, and 1, and it is easy to see that they map, respectively, onto $\eta = -1$, ∞, and 0. Consequently, the line $\mathrm{Im}s = 0$ maps onto the line $\mathrm{Im}\eta = 0$ with the orientation reversed. Thus we have shown that the half-plane $\mathrm{Im}s > 0$ is mapped by (23) onto the half-plane $\mathrm{Im}\eta < 0$.

We turn now to the branch of the square root in (22). Because we want $\mathrm{Re}\nu_\beta > 0$, we select the branch such that $-\pi/2 < \arg\nu_\beta < 0$. In summary, we have shown that the half-plane $\mathrm{Im}s > 0$ is mapped by (23) onto the half-plane $\mathrm{Im}\eta < 0$ which in turn is mapped by the square root in (22) onto the fourth quadrant, $-\pi/2 < \arg\nu_\beta < 0$. Note that we have also shown that real values of s such that $1/3 < s < 1$ map onto positive (real) values of ν_β and that real s with $s < 1/3$ or $s > 1$ give purely imaginary values of ν_β.

In our setting the stability theory may be summarized as follows.

(1) A zero of $F_q(s)$ in (18) with $\mathrm{Im}s > 0$ and with the branch of the square root as we just defined it is called a Godunov-Ryabenky mode, and it produces disastrous instability.

(2) Except for $s = 0$ a real zero of $F_q(s)$ in (18) outside the interval $1/3 \le s \le 1$ or outside the interval $1/(3q) \le s \le 1/q$ gives what is called a GKS instability. In making this statement, we have used the fact that the orientation is such that increasing real s corresponds to decreasing $\mathrm{Im}\nu$. It is Trefethen's insight [7] that a GKS mode corresponds to an infinite reflection coefficient, causing waves to arise spontaneously at the surface and propagate (undamped) into the medium. Trefethen also shows how to determine the group velocity of this downward propagation.

(3) If $q > 1/3$, a real zero of $F_q(s)$ in (18) such that $1/(3q) < s < 1$ is a Rayleigh wave. It just so happens that the GKS definition of stability is somewhat artificial in that, while it enables one to prove theorems, it also makes a Rayleigh wave unstable from the GKS point of view. The reason behind this state of affairs is that a small perturbation of the conditions which give rise to a Rayleigh wave may easily produce an instability in the more usual sense of unlimited growth of energy. In particular, the theory is still uncertain about the stability in the usual sense of Rayleigh waves in an inhomogeneous medium, although we expect no instability in the sense of energy growth.

We remark that in the stability theory Godunov-Ryabenky modes are regarded as easy special cases and that most of the mathematical effort is devoted to the marginal cases for which $\mathrm{Im}s = 0$.

The locations of the zeros of $F_q(s)$ with $s \neq 0$ for $q = 1/\sqrt{3}$ are given in Table I. Note that by squaring both terms on the right-hand side of (18) and clearing fractions, we get the product of s^4 with a polynomial in s of order eight. Thus, there are eight nonzero roots, but only the first two entries in the table are on the branch of interest to us, with $-\pi/2 \le \arg\nu_\alpha \le 0$ and $-\pi/2 \le \arg\nu_\beta \le 0$ and $\mathrm{Im}s \ge 0$. We remark that Table I could be enlarged, since $F_q(s)$ in (18) is unchanged if the branches are swapped whereby ν_α is replaced by $-\nu_\alpha$ and ν_β by $-\nu_\beta$. These exchanges produce no zeros on the branch we want.

The first two entries in Table I are Godunov-Ryabenky modes, and the GKS theory predicts exponential growth originating at the surface. The last two entries of Table I show that (18) has two real zeros with $s \neq 0$, but for neither of them is it true that both $\mathrm{Im}\nu_\alpha < 0$ and $\mathrm{Im}\nu_\beta < 0$. Thus, the 45° equation has no GKS modes. There are no Rayleigh waves since the real zeros do not satisfy the condition $1/\sqrt{3} < s < 1$.

VII. THE DIFFERENCE SCHEME

We now investigate a finite-difference approximation to the elastic paraxial equation (16) and study the effect of varying the mesh sizes. What is most interesting is the discretization may move the graph of $F_q(s)$ down until it intersects the s axis, like the shift to the *ad hoc* F_q in Fig. 1. We can even make one of the zeros of F_q lie on the Rayleigh root s_0. We will still have to get rid of the instability and the surface wave corresponding to the nonphysical zero of the discrete Rayleigh function. From the point of view of Table I what is happening is that the discretization may move one of the Godunov-Ryabenky modes onto the real axis, where it meets a zero from

TABLE I. Zeros of the 45° Rayleigh function.

s	$\beta\nu_\alpha/\omega$	$\beta\nu_\beta/\omega$
$0.408681 + 0.917218i$	$0.334197 - 0.809727i$	$0.404238 - 1.190657i$
$0.871022 + 0.0886209i$	$1.09803 - 0.220092i$	$0.574022 - 0.231059i$
$1.8475 + 0.00469868i$	$0.00371746 - 0.201036i$	$0.00105436 + 0.863881i$
$0.408681 - 0.917218i$	$0.334197 + 0.809727i$	$0.404238 + 1.190657i$
$0.871022 - 0.0886209i$	$1.09803 + 0.220092i$	$0.574022 + 0.231059i$
$1.8475 - 0.00469868i$	$0.00371746 + 0.201036i$	$0.00105436 - 0.863881i$
-0.92979	$-0.885978i$	$1.42725i$
0.310668	$-1.53910i$	$6.36795i$

another sheet. They then split into two Rayleigh modes. The other Godunov-Ryabenky mode remains and makes the method unstable.

Let us introduce a grid on the quadrant $x \geq 0$, $z \geq 0$ with mesh sizes h_x and h_z, so that a grid point is $(x_n, z_j) = (nh_x, jh_z)$ with integers $n \geq 0$ and $j \geq -1$. We also introduce the translation operators $T_x u(x,z) = u(x+h_x, z)$ and $T_z u(x,z) = u(x, z+h_z)$. Because we want a nondissipative difference scheme, we discretize the paraxial equation (16) as

$$\left(1 + \frac{\alpha^2}{4\omega^2 h_z^2}(T_z - 2 + T_z^{-1})\right) \frac{1}{h_x}(T_x - 1)\phi = i\omega \left(\frac{1}{\alpha} + \frac{3\alpha}{4\omega^2 h_z^2}(T_z - 2 + T_z^{-1})\right) \frac{1}{2}(T_x + 1)\phi, \tag{24a}$$

$$\left(1 + \frac{\beta^2}{4\omega^2 h_z^2}(T_z - 2 + T_z^{-1})\right) \frac{1}{h_x}(T_x - 1)\psi = i\omega \left(\frac{1}{\beta} + \frac{3\beta}{4\omega^2 h_z^2}(T_z - 2 + T_z^{-1})\right) \frac{1}{2}(T_x + 1)\psi. \tag{24b}$$

It is clear from (24) that there are two natural dimensionless parameters

$$\delta = \frac{\omega h_z}{\beta} \quad \text{and} \quad \theta = \frac{h_x}{h_z} \tag{25}$$

in addition to $q = \beta/\alpha$. The parameter δ is the reciprocal of the number of z-mesh points per wavelength of an S wave, so it is a measure of the resolution. Clearly, θ is the mesh ratio. In terms of these parameters (24) takes the form

$$\left(1 + \frac{1}{4q^2\delta^2}(T_z - 2 + T_z^{-1})\right)(T_x - 1)\phi = i\left(q\delta + \frac{3}{4q\delta}(T_z - 2 + T_z^{-1})\right)\frac{\theta}{2}(T_x + 1)\phi, \tag{26a}$$

$$\left(1 + \frac{1}{4\delta^2}(T_z - 2 + T_z^{-1})\right)(T_x - 1)\psi = i\left(\delta + \frac{3}{4\delta}(T_z - 2 + T_z^{-1})\right)\frac{\theta}{2}(T_x + 1)\psi. \tag{26b}$$

This difference scheme is applied at the grid points (nh_x, jh_z) with $n \geq 0$ and $j \geq 0$.

VIII. THE DISCRETE DISPERSION RELATION

For the difference scheme (26) in place of (9) it is more convenient to obtain the dispersion relation by searching for solutions of the form

$$\phi(nh_x, jh_z) = A\xi^n \zeta_\alpha^j, \qquad \psi(nh_x, jh_z) = B\xi^n \zeta_\beta^j. \tag{27}$$

A direct calculation gives the dispersion relation for discrete P waves,

$$\zeta_\alpha + \frac{1}{\zeta_\alpha} = 2 - 4\left(\frac{q\delta\theta(\xi+1) + 2i(\xi-1)}{3q\delta\theta(\xi+1) + 2i(\xi-1)}\right) q^2\delta^2. \tag{28}$$

Similarly, the dispersion relation for discrete S waves is

$$\zeta_\beta + \frac{1}{\zeta_\beta} = 2 - 4\left(\frac{\delta\theta(\xi+1) + 2i(\xi-1)}{3\delta\theta(\xi+1) + 2i(\xi-1)}\right)\delta^2. \tag{29}$$

For $\delta = 0$ (zero frequency) these mappings become trivial, giving $\zeta_\alpha = \zeta_\beta = 1$ for all values of ξ. We therefore require that $\delta \neq 0$.

IX. THE DISCRETE RAYLEIGH FUNCTION

As a discretization of the boundary condition (8) at surface grid points $(nh_x, 0)$ with $n \geq 0$ we use

$$\frac{2}{\theta}(T_x - 1)(T_z - T_z^{-1})\phi + (T_x + 1)\left[\delta^2 + 2(T_z - 2 + T_z^{-1})\right]\psi = 0, \tag{30a}$$

$$\left[(2q^2 - 1)\delta^2 + 2(T_z - 2 + T_z^{-1})\right](T_x + 1)\phi - \frac{2}{\theta}(T_x - 1)(T_z - T_z^{-1})\psi = 0, \tag{30b}$$

where we have used (7) to eliminate ∂_x^2. Thus, both (26) and (30) make use of the values of ϕ and ψ at the supplementary grid point $(nh_x, -h_z)$. If we substitute the modal solution (27) into the discrete boundary condition (30), we find that nontrivial solutions exist if and only if

$$\det \begin{pmatrix} M & N \\ P & Q \end{pmatrix} = 0, \tag{31}$$

where the entries are given by

$$M = \frac{2}{\theta}(\xi - 1)\left(\zeta_\alpha - \frac{1}{\zeta_\alpha}\right), \tag{32a}$$

$$N = (1+\xi)\delta^2 + \left\{2\left(\zeta_\beta - 2 + \frac{1}{\zeta_\beta}\right)\right\}, \tag{32b}$$

$$P = (1+\xi)\left\{(2q^2 - 1)\delta^2 + 2\left(\zeta_\alpha - 2 + \frac{1}{\zeta_\alpha}\right)\right\}, \tag{32c}$$

$$Q = -\frac{2}{\theta}(\xi - 1)\left(\zeta_\beta - \frac{1}{\zeta_\beta}\right). \tag{32d}$$

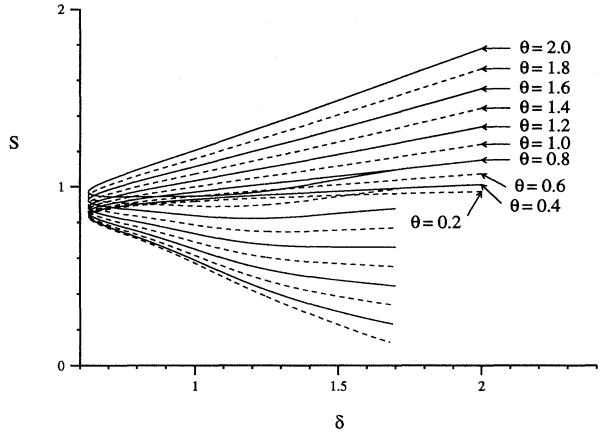

FIG. 2. Discrete Rayleigh wave speeds.

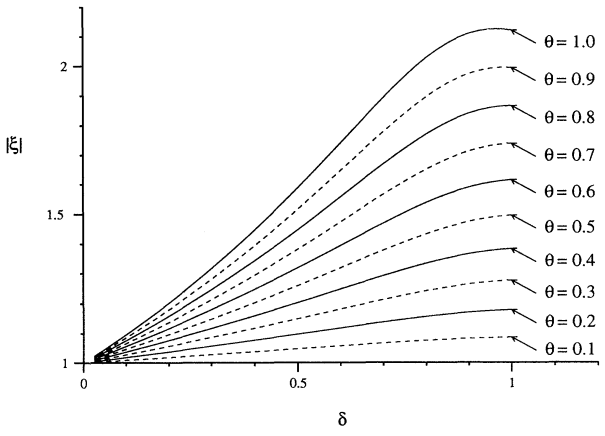

FIG. 3. Unstable discrete mode.

The correspondence between the modes (9) and (27) is that

$$\xi = \exp\{ikh_x\}, \quad \zeta_\alpha = \exp\{-\nu_\alpha h_z\}, \quad \zeta_\beta = \exp\{-\nu_\beta h_z\}. \tag{33}$$

We might therefore reasonably expect that for $|\xi| = 1$ the discrete Rayleigh function $MQ - NP$ should behave like the 45° Rayleigh function (18) as the mesh sizes get smaller, $\delta \to 0$. We have computed the zeros of the determinant (31) for several values of δ and mesh ratio θ. In Fig. 2 we display the ratio $S = \delta\theta/\arg\xi$ for these zeros ξ. The reason for plotting this ratio is that by (33) we have $S = \omega/(k\beta)$, so that S is the ratio of the Rayleigh wave speed ω/k to the S-wave speed β. The figure shows that the discrete 45° equation (26) has two Rayleigh waves with $|\xi| = 1$, $\mathrm{Re}\zeta_\alpha > 0$, and $\mathrm{Re}\zeta_\beta > 0$ only if δ is larger than about 0.63. Since δ is 2π divided by the number of z points per wavelength, this means that there are discrete Rayleigh waves only if there are ten or fewer points per wavelength in the z direction. The high speed S of the discrete Rayleigh wave for large values of θ is surprising—it can go faster than a P wave.

X. STABILITY

In order to apply the GKS theory to the difference scheme (26) with the boundary condition (30), we investigate (28) and (29) as conformal mappings of the region $|\xi| > 1$. It suffices to consider (29), and we see that it is the composition of a fractional linear transformation with a translation and scaling $w = 2 - 4\delta^2 z$ and a Zhukovsky transformation

$$\zeta_\beta + \frac{1}{\zeta_\beta} = w. \tag{34}$$

For an analysis of the Zhukovsky transformation see Bieberbach [8]. We take the branch of (34) such that $|\zeta_\beta| \le 1$ since we require solutions to be bounded with increasing depth. By going through this chain of mappings, it is easy to show that the region $|\xi| > 1$ is mapped by (29) onto the half-disk $|\zeta_\beta| < 1$ and $\mathrm{Im}\zeta_\beta > 0$. Furthermore, (28) puts ζ_α in the same half-disk.

The GKS theory again has three cases. (1) If the determinant (31) has a zero in $|\xi| > 1$, it is a Godunov-Ryabenky mode which is unstable with exponential growth. (2) If the determinant (31) has a zero on the circle $|\xi| = 1$ with $|\zeta_\alpha| = 1$ or $|\zeta_\beta| = 1$, there is a GKS instability with waves propagating undamped into the medium. (In making this statement, we have used the fact that clockwise motion along the circle $|\xi| = 1$ corresponds to counterclockwise motion on $|\zeta| = 1$.) (3) If (31) has a zero $|\xi| = 1$ with $-1 < \zeta_\alpha < 1$ and $-1 < \zeta_\beta < 1$, then there is a discrete Rayleigh wave. Again, a discrete Rayleigh wave is unstable according to the GKS definition of stability, but in fact we do not expect it to exhibit energy growth.

Our computations of the solutions of (31) indicate the presence of a Godunov-Ryabenky instability, and its magnitude is shown in Fig. 3 as a function of the parameters δ and θ defined in (25). We have already noted the presence of discrete Rayleigh waves if δ is not too small. Our computations indicate that as δ is decreased past where the roots in Fig. 2 merge, they bifurcate into a pair with one of them stable $|\xi| < 1$, and the other is another Godunov-Ryabenky mode. This unstable mode has $|\xi|$ smaller than that shown in Fig. 3, however.

The effect of the unstable mode is evident in Fig. 4, where we show contours of $\log_{10}|\psi|$ for the solution of

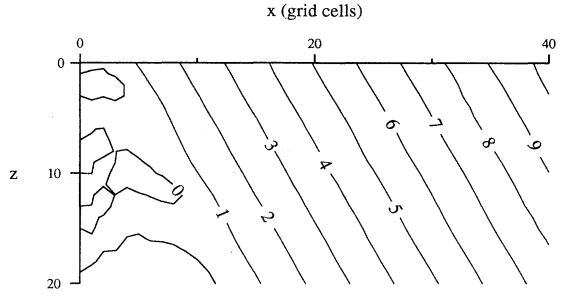

FIG. 4. Contour levels of $\log_{10}|\psi|$.

(26) with boundary condition (30) at $z = 0$. In this figure we have taken the orientation as is common in seismology with the positive x axis going to the right and the positive z axis going down. The initial data for Fig. 4 are that $\phi = \psi = 1$ at $x = 0$, and the boundary conditions at the bottom of the figure are discretizations of $\partial_z\phi = \partial_z\psi = 0$. As values of the parameters in the difference scheme we chose $q = 1/\sqrt{3}$, $\delta = 2/3$, and $\theta = 1$. The reason for this choice of parameters is that according to Fig. 2, they give a Rayleigh wave of nearly correct speed. (And they also give a slower Rayleigh wave.) It is clear in Fig. 4 that the instability is initiated at the free surface and that it propagates downward. It is also easy to show that the rate of growth is as predicted by Fig. 3.

XI. SOME COMPUTATIONAL DETAILS

We have so far talked about the difference scheme (26) with boundary condition (30) as if the domain extended to infinite depth $0 < z < \infty$, but in any actual computation we must truncate at some value $z = z_J$ and supply some sort of boundary condition there. We have tried several arbitrary bottom boundary conditions, including the Dirichlet condition

$$\phi = \psi = 0 \text{ at } z = z_J,$$

a discrete Neumann condition

$$(T_z - T_z^{-1})\phi = (T_z - T_z^{-1})\psi = 0 \text{ at } z = z_J,$$

and an extrapolation of the discrete Rayleigh wave solution (27). On computational grounds there is not much difference in the effects of these bottom boundary conditions, but we prefer the Rayleigh-wave extrapolation because it is more physically realistic.

As mentioned in the Introduction, the difference scheme (26) with a discrete free surface condition (30) and a bottom boundary condition produce a matrix problem (1) at each propagation step

$$\mathcal{N}V_n = \mathcal{M}V_{n-1},$$

where V_n is a vector of the grid values of ϕ and ψ at distance $x = x_n$ from the start. It is useful to think of the removal of undesirable modes in terms of an expansion in eigenvectors

$$U = \sum_m c_m V(m), \tag{35}$$

where $V(m)$ satisfies

$$\xi_m \mathcal{N}V(m) = \mathcal{M}V(m). \tag{36}$$

The free-surface boundary condition (30) makes the matrices $\mathcal{M}$ and $\mathcal{N}$ non-self-adjoint, so that in order to compute the coefficients c_m in (35), we need the left eigenvectors $W(m)$,

$$\xi_m [W(m)]^T \mathcal{N} = [W(m)]^T \mathcal{M}. \tag{37}$$

The eigenvectors $W(m)$ and $V(m)$ satisfy a weighted biorthogonality relation, and we may normalize them so that

$$[W(l)]^T \mathcal{N} V(m) = \delta_{lm}. \tag{38}$$

It follows from (38) that the coefficient c_m in (35) is given by

$$c_m = [W(m)]^T \mathcal{N} U,$$

so that we may remove an unstable mode $V(1)$ from U by using the operation

$$U \mapsto U - \{[W(1)]^T \mathcal{N} U\} V(1). \tag{39}$$

The operation (39) is known in numerical linear algebra as deflation. See Wilkinson [4]. Wilkinson points out that deflation is numerically unreliable if one tries to use it to remove too many eigenvectors, but we remove only two: the unstable mode and the nonphysical discrete Rayleigh wave. Numerical errors involved with each mode removal introduce small contributions of eigenvectors that were previously removed. For this reason at each propagation step we first remove the nonphysical Rayleigh wave and then the unstable mode, in order to be sure to keep out the instability.

We remark that we have presented the biorthogonality in its usual form (38), but it follows from (36) and (37) that we could replace it by

$$[W(l)]^T \mathcal{M} V(m) = \delta_{lm}. \tag{40}$$

Numerically, the effects of using (40) in place of (38) are significant for eigenvalues $\xi_m \approx 0$, but we have observed only small differences in computed results. For computational reasons the biorthogonality (40) is more convenient because for the iteration scheme (1) we keep a copy of the matrix $\mathcal{M}$, but we keep only a factored form of $\mathcal{N}$ obtained by Gaussian elimination.

XII. CONCLUSION

We want to emphasize that the computation of Rayleigh waves is extremely delicate because they are only marginally stable. In fact, they are unstable in the GKS sense of stability. Thus, any perturbation by using a paraxial approximation or even finite differences or finite elements can easily make Rayleigh waves either die out or become unstable. In the cases we considered here, they happen to become unstable.

Although it is true that the 45° equation has no Rayleigh waves, we have seen that its discretization does have them if the mesh size is sufficiently coarse. The requirement of a coarse mesh is not as strange as it may seem. In fact, one of the advantages of paraxial equations is that because they may be derived from a coordinate system moving with the wave [1], discretizaton of a paraxial equation may give sufficient accuracy on a coarser grid than would be required for the full wave equation (7). Furthermore, the curves in Fig. 2 show that

the vertical resolution δ and the mesh ratio θ may be chosen so that the difference scheme has Rayleigh waves of the proper speed. The nonphysical discrete Rayleigh wave may be removed by the same kind of projection as is used to remove the unstable mode.

Note also that we have not dealt with all of the difficulties related to horizontal elastic paraxial equations. In particular, we have treated the frequency ω as fixed, but one would normally either use a space-time paraxial equation or (more likely) solve the equations (7) for a large number of frequencies and compute the time-dependent solution by a discrete Fourier transform over ω. Our method requires, however, that the mesh parameters δ and θ given by (25) be constant. That is, one would have to vary the mesh sizes h_x and h_z so as to keep ωh_x and ωh_z constant. This greatly complicates the Fourier synthesis.

Finally let us note that we have applied the boundary condition (8) of zero normal traction to the elastic paraxial equation (16), and that this has created some difficulties. Although this boundary condition is appropriate for the elastic equation (5), there is no physical reason to require it for (16). We have not investigated the effects of modifying the boundary condition. We merely wish to point out that it is not sacrosanct.

ACKNOWLEDGMENTS

The author wishes to thank David Harris and Shawn Larsen for their valuable comments. Furthermore, we thank Shawn Larsen for permitting us to use his computer program as a basis for our modifications. This work was supported by the Applied Mathematical Sciences subprogram of the Office of Energy Research, U.S. Department of Energy, by Lawrence Livermore National Laboratory under Contract No. W-7405-Eng-48.

[1] J. Claerbout, *Imaging the Earth's Interior* (Blackwell Scientific, Palo Alto, California, 1985).
[2] R. W. Graves, Ph. D. thesis, California Institute of Technology (1991) (unpublished).
[3] C. P. A. Wapenaar, *Elastic Wavefield Extrapolation* (Elsevier, New York, 1989).
[4] J. H. Wilkinson, *The Algebraic Eigenvalue Problem* (Clarendon Press, Oxford, 1965).
[5] J. A. Hudson, *The Excitation and Propagation of Elastic Waves* (Cambridge University Press, Cambridge, England, 1980).
[6] B. Gustafsson, H.-O. Kreiss, and A. Sundström, Math. Comp. **26**, 649 (1972).
[7] L. N. Trefethen, Comm. Pure Appl. Math. **37**, 329 (1984).
[8] L. Bieberbach, *Conformal Mapping* (Chelsea, New York, 1953).